Superimposed Positive Sequence Impedance for Detecting Unintentional Islanding in Microgrid

Indradeo Pratap Bharti[1,*], Navneet Kumar Singh[1], Om Hari Gupta[2], Asheesh Kumar Singh[1] and Vijay K. Sood[3]

[1]*MNNIT Allahabad, Prayagraj, India*
[2]*NIT Jamshedpur, Jamshedpur, India*
[3]*Ontario Tech University, Oshawa, ON, Canada*
E-mail: Indradeo.2019ree12@mnnit.ac.in; navneet@mnnit.ac.in; omhari.ee@nitjsr.ac.in; asheesh@mnnit.ac.in; vijay.sood@ontariotechu.ca
[*]*Corresponding Author*

Received 20 September 2023; Accepted 15 March 2024

Abstract

Incorporation of environmentally friendly energy sources (RESs) into the electricity grid has many benefits, including economic, technological, and environmental. However, excessive renewable energy sources (RES) in the power grid provide technical problems, including equipment protection, DG operation, and islanding detection. One of the most serious challenges is the islanding phenomenon. Islanding can cause several problems, such as frequency instability and voltage fluctuations resulting in damage to electrical equipment or threatening utility workers who may be working/accessing the equipment. This research proposes an efficient islanding detection algorithm to lessen the impact of such threats. This novel passive islanding detection scheme is based on superimposed positive sequence impedance (SPSI). For calculating the superimposed positive sequence impedance (SPSI), the

Distributed Generation & Alternative Energy Journal, Vol. 39_3, 559–592.
doi: 10.13052/dgaej2156-3306.3938

voltage and current signals are obtained from targeted DG points. The scheme's performance is tested on multiple bus systems across islanding and non-islanding conditions using a MATLAB/Simulink environment. It is shown that even in the presence of noise, the algorithm can determine an islanding decision with high accuracy and a short detection time of 84 ms. In comparison to other algorithms, it operates at zero power mismatch (ZPM) and does not affect power quality.

Keywords: Multi-bus network, islanding detection, SPSI, synchronous DG, microgrid, wind energy conversion.

Abbreviation

PCC	–	Point Common Coupling
DWT	–	Discrete wavelet transform
TMF	–	Transient monitoring function
ROCONSV	–	Rate of change of negative sequence voltage
ROCOV/ROCOAP	–	Rate of change of voltage and active power

1 Introduction

1.1 Motivation

In the present era of rising energy consumption, the efficient and reliable operation of the power grids with the formation of microgrids (fed from distributed and clean energy sources such as solar power, and wind power and often supported by battery storage) has become increasingly important. These microgrids improve power quality as well as reduce system losses to enhance system performance and reliability. However, the widespread use of distributed energy sources has led to a few difficulties such as harmonic injection and control, islanding detection, voltage flickers, and coordination of multiple DGs [1, 2]. When microgrids are integrated into electric power systems, islanded operation, and islanding detection are major concerns. There are two types of islanding: intentional islanding and unintentional islanding. Unintentional islanding is one of the most significant hazards impacting microgrids. Islanding detection techniques are used to detect unintentional island formation when the microgrid separates from the power grid in the case of an abnormal condition. Due to these disadvantages, the IEEE-1547 guideline requires islanding detection within two seconds and disconnection of distributed generators (DGs) from the electrical system [3].

1.2 Literature Review

From the motivation section, inadvertent islanding identification is a critical problem in microgrid systems. Therefore, several islanding techniques have been designed to identify islanding events. However, most existing methods suffer from various drawbacks such as a wide non-detection zone, degraded power quality, and difficulty in determining thresholds. Whereas the suggested islanding strategy successfully overcomes the aforementioned issues. This literature review provides an overview of the various islanding detection approaches, such as local and remote techniques shown in Figure 1, along with the benefits and drawbacks of centralized and decentralized systems [4]. Three types of local schemes exist active, passive, and hybrid.

Passive Islanding Algorithms

Passive islanding detection approaches detect islanding by monitoring local characteristics like frequency, voltage, THD, and power factor at the PCC. While the distributed power system works in islanded mode, the local parameters exceed a specified limit. If an islanding event is detected, the system will immediately trip the DER's circuit breaker, reducing the risk of system damage. Passive islanding detection is a critical safety measure that can help ensure the grid's reliability and safety. The benefits of passive approaches involve simple execution and no risk of power quality issues. The main challenge is the large NDZ and threshold selection [5]. Some examples of passive techniques are voltage vector shift, harmonic monitoring, rate of change of frequency, over/under voltage and frequency deviation, positive sequence superimposed [6], and rate of change of frequency. Advanced intelligence and signal processing algorithms solve a technical challenge that happens in passive approaches and improve their effectiveness, such as NDZ reduction and increased efficiency for islanding detection. Several approaches based on fuzzy logic, artificial neural networks, decision trees, Naive Bayesian classifiers, and Random Forest classifiers have been established in the literature [7, 8].

Active Islanding Algorithms

Active islanding methodologies work when perturbation signals are fed into the system, causing variations in local parameters under abnormal circumstances to be acquired at the PCC. If a microgrid is tied to the electrical grid, there are no significant deviations in local characteristics. In islanded mode,

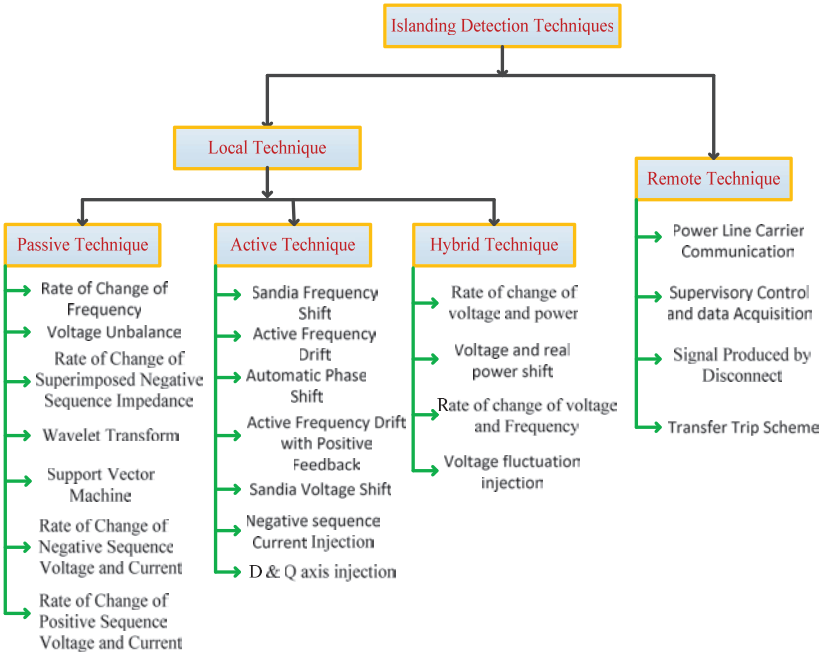

Figure 1 Organization of islanding detecting methodologies.

local parameter variations are greater than the threshold. These approaches have nearly little NDZ as compared to passive systems [9]. This disturbance can affect the power quality of the distribution system in both grid-connected and islanding modes. Due to the disadvantages of each technique, neither could be completely effective. A few examples of active methods are Active Frequency Drift (AFD), Impedance Measurement, and D-axis and Q-axis current injection.

Hybrid Islanding Methods

Hybrid islanding detection approaches use both passive and active strategies [10, 11]. Passive approaches have a wide NDZ, but active methods suffer from power quality difficulties caused by disturbance signals injected into the system. As a result, hybrid techniques are being developed to address these issues. Some examples of hybrid techniques are the average rate of voltage change and actual power shift, the rate of change in reactive power and load connection strategy, the ROCOV and ROCORP with capacitor connection, and the load shedding technique.

Remote Islanding Algorithms

In remote islanding detection methods, a link is needed for interaction between the power grid and the microgrid. Remote techniques have zero non-detection zone (NDZ) and are highly reliable [12]. The main drawback of a remote scheme is the high cost of installation. Examples of remote schemes include power line carrier communication (PLCC) [13], supervisory control and data acquisition method (SCADA) [14], signals produced a disconnect (SPD) [15], transfer trip schemes, impedance insertion method, and phasor measurement unit (PMU) [16].

1.3 Contribution and Organization of this Article

To summarize, passive islanding detection methodologies are ineffective when the power generating unit and the load's demand are equal. The passive scheme has a large NDZ. Nonetheless, active schemes overcome this issue as well, but they deteriorate network power quality by injecting unnecessary signals. Remote approaches are more costly, and their adoption in electrical systems is highly complicated. Hybrid approaches require a long detection time and are difficult to calculate. A novel passive approach can overcome these challenges and work with zero power mismatch. This methodology has been demonstrated on a converter and synchronous-based multi-bus network under several islanding and non-islanding events. The following contributions of the suggested approach are given below:

- It accurately and quickly identifies islanding without degrading power quality.
- It operates at zero NDZ.
- It is reliable and easy to apply for converters and synchronous-based DGs.
- The proposed approach detects islanding as well as distinguishing it from grid faults.
- The process of determining threshold values is simple.
- This scheme is superior to the conventional passive technique.
- The suggested method can identify islanding under balanced conditions.
- It performs very well in both noisy and DG-tripping conditions.

The other part of the paper is structured as follows: the proposed approach and its process diagram are presented in Section 2. Section 3 describes the multi-bus network. Section 4 contains a summary of the simulation results. Section 5 contains a comparative study. The paper's conclusion is found in Section 6.

2 Proposed Methodology

2.1 The Proposed Scheme Models

This research aims to provide a novel passive approach using superimposed positive sequence impedance to detect islanding occurrences in the microgrid test system. The voltage and current signals are monitored at the DG terminal. The harmonics from the voltage and current signal are extracted using a full-cycle Discrete Fourier Transform (DFT).

Let X(t) be the continue signal, w is the angular frequency, t is time, X_p is the peak value of the signal, and θ is the angle.

$$X(t) = X_p Sin(wt + \theta) \tag{1}$$

A sampling of signal

$$X_n(t) = X_p Sin(wt_n + \theta) \tag{2}$$

Where, $t_n = n\Delta t$; n = 0, 1, 2…,
Δt = Time interval between successive samples
Phasor estimation: 1-cycle DFT

Applying 1-cycle DFT on signal is given in Equation (1)

$$\text{Signal phasor, } \dot{X}(t) = \frac{\sqrt{2}}{N} \sum_{n=0}^{N-1} \left(X_n e^{-\frac{j2\Pi n}{N}} \right) \tag{3}$$

$0 \leq$ n $\leq$ N-1 where, N = Number of samples in a cycle $X_n = n^{th}$ sample of X(t).

Calculate the real and imaginary parts of the signal X(t) using Equation (3).

The real coefficient of signal

$$X_{real} = \frac{\sqrt{2}}{N} \sum_{n=0}^{N-1} \left[X_n Cos \left(\frac{2\pi n}{N} \right) \right] \tag{4}$$

Imaginary coefficient of signal

$$X_{imag} = \frac{\sqrt{2}}{N} \sum_{n=0}^{N-1} \left[X_n Sin \left(\frac{2\pi n}{N} \right) \right] \tag{5}$$

Computed phasor;

$$\dot{X} = X_{real} - jX_{imag} = |X| \angle \theta$$

Estimate the magnitude and phase angle of the signal using Equations (4) and (5).

$$|X| = \sqrt{X_{real}^2 + X_{imag}^2},\ \theta = -\tan^{-1}\left(\frac{X_{imag}}{X_{real}}\right)$$

Equations (6) and (7) can be used to calculate pre- and past-islanding event voltage and current at the DG terminal for estimated superimposed voltage ΔV_{DG} and current ΔI_{DG}.

$$\Delta V_{DG} = V_{DG\_Post} - V_{DG\_Pre} \tag{6}$$

$$\Delta I_{DG} = I_{DG\_Post} - I_{DG\_Pre} \tag{7}$$

Estimate sequence component of voltage and current.

The phasor components of voltage ($\Delta \mathrm{V_a}$, $\Delta \mathrm{V_b}$, and $\Delta \mathrm{V_c}$) and current ($\Delta \mathrm{I_a}$, $\Delta \mathrm{I_b}$, and $\Delta \mathrm{I_c}$) are obtained from DFT. The sequence analyzer transfers phase quantity into sequence components of voltage ($\Delta \mathrm{V}_0$, $\Delta \mathrm{V}_1$, and $\Delta \mathrm{V}_2$) and ($\Delta \mathrm{I}_0$, $\Delta \mathrm{I}_1$, and $\Delta \mathrm{I}_2$) using Equations (8), and (9). A fault in the main grid or DG will cause the zero sequence components to appear. During islanding or fault switching, negative sequence components are present. All modes will contain the positive sequence components [17].

$$\begin{bmatrix}\Delta V_0\\ \Delta V_1\\ \Delta V_2\end{bmatrix} = \frac{1}{3} \times \begin{bmatrix}1 & 1 & 1\\ 1 & m & m^2\\ 1 & m^2 & m\end{bmatrix} \times \begin{bmatrix}\Delta V_a\\ \Delta V_b\\ \Delta V_c\end{bmatrix} \tag{8}$$

$$\begin{bmatrix}\Delta I_0\\ \Delta I_1\\ \Delta I_2\end{bmatrix} = \frac{1}{3} \times \begin{bmatrix}1 & 1 & 1\\ 1 & m & m^2\\ 1 & m^2 & m\end{bmatrix} \times \begin{bmatrix}\Delta I_a\\ \Delta I_b\\ \Delta I_c\end{bmatrix} \tag{9}$$

where, $m = 1\angle 120^\circ$ is the complex operator.

$$\Delta V_1 = \frac{1}{3}(\Delta V_a + \Delta V_b m + \Delta V_c m^2) \tag{10}$$

$$\Delta I_1 = \frac{1}{3}(\Delta I_a + \Delta I_b m + \Delta I_c m^2) \tag{11}$$

Superimposed positive sequence impedance (SPSI) is calculated using Equations (10) and (11).

$$SPSI = \left|\frac{V_{1Post} - V_{1Pre}}{I_{1Post} - I_{1Pre}}\right| = \left|\frac{\Delta V_1}{\Delta I_1}\right| = |\Delta Z_1| \tag{12}$$

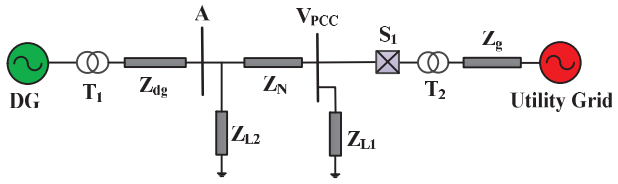

Figure 2 The graphical representation of a distribution system.

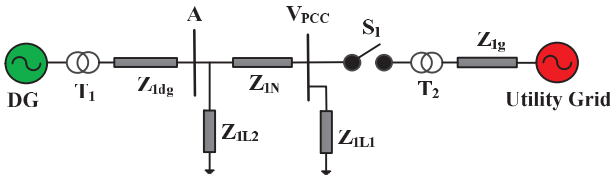

Figure 3 System diagram in the islanding mode.

Calculate the absolute mean of SPSI using Equation (13)

$$ASPSImean = \frac{1}{T}\int_{t-T}^{t} |\Delta Z_1| dt \tag{13}$$

Where T represents a fundamental period and t is instantaneous time.

2.2 The Proposed Algorithm Study Under Various Scenarios

A distribution system test model is used to analyze the proposed protection scheme. In this network, converter and synchronous based-DGs and loads interface with the power grid at the PCC, as shown in Figure 2 where switch S_1 determines the operating mode of the microgrid network.

2.2.1 The distribution system is operated in islanding mode

According to Figure 3, switch S_1 is open, and the distributed test system is operating in islanding mode. The equivalent positive sequence impedance can be viewed from the DG terminal, as shown in Figure 4.

The following Kirchhoff's voltage law (KVL) equations are applied to the test network as depicted in Figure 4.

$$\Delta V_A - Z_{1N}\Delta I_1 - Z_{1L1}\Delta I_1 = 0 \tag{14}$$

$$\Delta V_A - Z_{1L2}\Delta I_2 = 0 \tag{15}$$

$$\Delta I_{1dg} = \Delta I_1 + \Delta I_2 \tag{16}$$

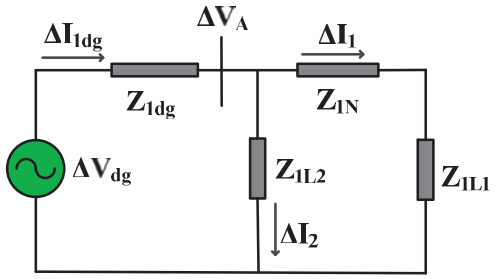

Figure 4 The equivalent circuit diagram of the system viewed from the DG during an islanding event.

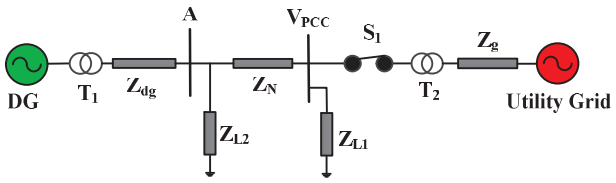

Figure 5 System diagram in the grid-connected mode.

$$\Delta I_{1dg} = \frac{\Delta V_A}{Z_{1N} + Z_{1L1}} + \frac{\Delta V_A}{Z_{1L2}} \tag{17}$$

$$\Delta Z_{1A}(th) = \frac{\Delta V_A}{\Delta I_{1dg}} = [Z_{1L2}||[Z_{1N} + Z_{1L1}]] \tag{18}$$

Where ΔV_{dg} and ΔV_g denote the DG and grid superimposed voltages respectively. ΔI_{1dg} denotes the superimposed positive sequence current of DG. Z_{1dg} and Z_{1N} represent the positive sequence impedance (PSI) of the DG and distribution line, respectively. The positive sequence impedances of the Loads L_2 and L_1 are indicated by Z_{1L2} and Z_{1L1} respectively.

2.2.2 The distribution network is operating in grid-tied mode.

When switch S_1 is closed, the microgrid is operated in grid-connected mode, as shown in Figure 5. The equivalent positive sequence impedance at the DG terminal is calculated from Figure 6.

The Kirchhoff's voltage law (KVL) equations utilized in the test network in Figure 6 are indicated below:

$$\Delta V_A - Z_{1N}\Delta I_1 - Z_{1L1}\Delta I_1 - Z_{1L1}\Delta I_{1g} = 0 \tag{19}$$

$$\Delta V_g - Z_{1g}\Delta I_{1g} - Z_{1L1}\Delta I_1 - Z_{1L1}\Delta I_{1g} = 0 \tag{20}$$

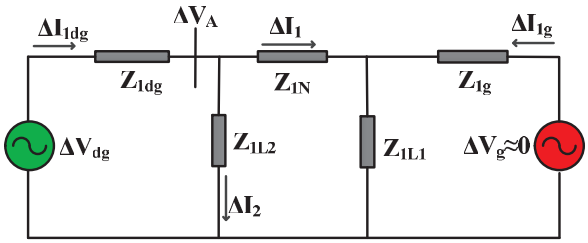

Figure 6 The equivalent circuit diagram of the distribution network during a non-islanding event.

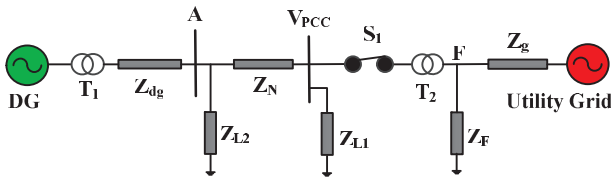

Figure 7 System diagram of the fault condition.

In grid-connected mode, the superimposed grid voltage is approximately zero (ΔVg $\approx$ 0).

$$[Z_{1g} + Z_{1L1}]\Delta I_{1g} + Z_{1L1}\Delta I_1 = 0 \tag{21}$$

$$\Delta V_A - Z_{1L2}\Delta I_2 = 0 \tag{22}$$

$$\Delta Z_{1A}(th) = \frac{\Delta V_A}{\Delta I_{1dg}} \tag{23}$$

$$\Delta Z_{1A}(th) = \frac{\Delta V_A}{\Delta I_{1dg}} = [Z_{1L2}||[Z_{1N} + [Z_{1L1} \parallel Z_{1g}]]] \tag{24}$$

2.2.3 The small power plant worked in a grid-linked state when faults occurred

The positive sequence impedance (PSI) at the DG terminal is determined by a fault at point F, as shown in Figure 7. Figure 8 shows the equivalent circuit diagram of a grid-connected system during a fault.

$$\Delta Z_{1A}(th) = [Z_{1L2}||[Z_{1N} + [Z_{1L1} \parallel [Z_{1F} \parallel Z_{1g}]]]] \tag{25}$$

Where positive sequence fault impedance is indicated by Z_{1F} and superimposed fault current is denoted by ΔI_F.

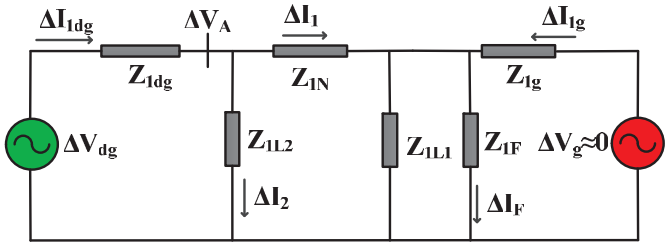

Figure 8 Microgrid's grid-connected mode and related circuits when a fault occurs.

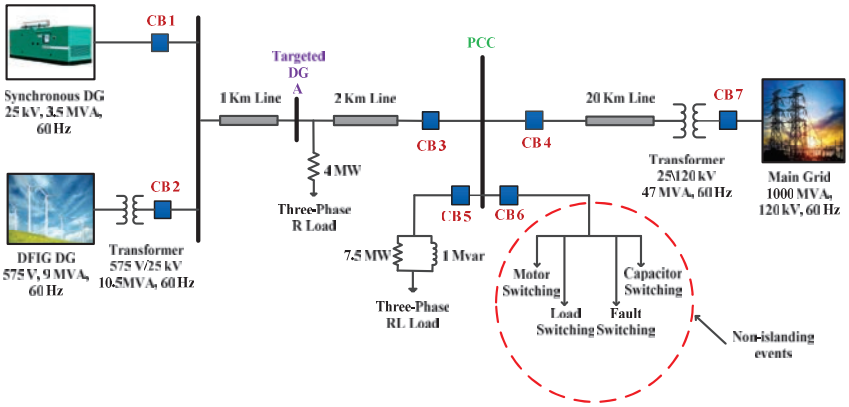

Figure 9 Simulink model of the microgrid.

Three cases of the distribution system are discussed above. An islanding mode has a higher equivalent positive sequence impedance than a grid-connected mode. Therefore, the variation in superimposed positive sequence impedance is more than the positive sequence impedance in the islanding event.

3 Model of a Test System

The proposed scheme tested on the multi-bus network for islanding detection is modeled in a MATLAB environment. Figure 9 depicts the multi-bus test network, which includes a DFIG wind farm (DG-1), a diesel generator (DG-2), local loads (L_1, L_2), and transmission lines. The small electrical system is linked to the power grid via a switch. Table 1 summarizes the Simulink parameters of the test system. The distributed power system operates at a frequency of 60 Hz and a voltage of 120 kV. The circuit breaker

Table 1 A description of the test network's parameters

S.N.	Parameters	Type	Value
1.	Utility Grid	Generation (swing)	120 kV, 1000 MVA, 60 Hz
2.	Wind turbine (DFIG)	Distributed generation	575 V, 9 MW, 60 Hz
3.	Diesel Synchronous Generator		25 kV, 3.5 MVA, 60 Hz
4.	Transformer (T_1)	Step-down	120/25 kV, 47 MVA, 60 Hz
5.	Transformer (T_2)	Step-up	0.575/25 kV, 10.5 MVA, 60 Hz
6.	Distribution Line	π line Model	1, 2, 20 km
7	Three Phase Load	Z constant impedance	4, 7.5 MW, 1 MVA

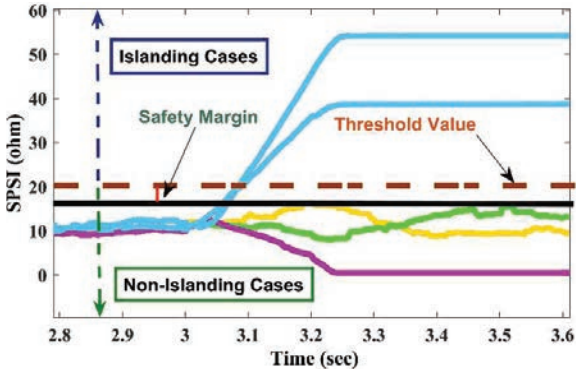

Figure 10 Comparison of detection parameters SPSI in both islanding and non-islanding scenarios.

(CB) decides the state of operation of the test network. When the (CB) is opened, the microgrid operates in stand-alone mode; when the CB is closed, the microgrid operates in grid-connected mode.

3.1 Setting a Threshold for the Proposed Method

There are several factors to consider when setting the threshold for the islanding detection index (IDI), such as the size of the system, network parameters, and the capacity of the DGs. It is achieved by simulating various islanding and non-islanding events and analyzing their parameters within permissible limits by varying generations, loads, fault resistances, voltages, currents, and impedances. It has been noticed that the average value of SPSI rises sometimes but remains less than 16 Ω in non-islanding scenarios. However, the average SPSI value remains above 54 Ω in the islanding case, as demonstrated in Figure 10. To avoid cascaded tripping of the DGs, an optimal

threshold of 20 Ω is selected to be lower than the smallest amount of average SPSI in an islanding scenario and higher than the highest amount of SPSI in a non-islanding scenario.

4 Results and Discussion

A multi-bus microgrid is used to verify the proposed approach and assess its effectiveness, as shown in Figure 9. The suggested islanding detection methodology is evaluated under two different working scenarios: (1) an islanding case and (2) a non-islanding case. For both cases the following tests are carried out: a fault, sudden load connection, and capacitor switching, noise in grid connection mode. Various comparisons of the proposed scheme to existing passive islanding detection methods are also performed.

4.1 Islanding Events

4.1.1 Positive power mismatch islanding condition

The performance of the proposed scheme is verified on various positive power mismatches (0%, 25%, and 75%) between the sum of distributed generation power and load demand. As seen in Figure 11(a), islanding is detected when the SPSI magnitude variation exceeds the threshold value (20 Ω). A trip signal is sent to the DG unit breaker when an islanding situation occurs. In the case of a circuit breaker that opens at 3 s and detects islanding after 0.082 s, as shown in Figure 11(b).

4.1.2 Negative power mismatch islanding condition

When generation power is higher than load demand, the proposed scheme is tested on different levels of negative power mismatch (−10%, −20%, and −30%). According to Figure 12(a), the response of the SPSI in various cases exceeds the threshold limit. In this case, the suggested technique detects islanding and produces a trip signal for circuit breaker operation, as shown in Figure 12(b). This method is more effective in all power mismatch situations and can quickly identify an islanding event.

4.1.3 Quality factor condition

The Quality factor is also defined as the ratio of the reactive power of the capacitor or inductor to the average power of the resistor at resonance. The quality factor of the load range lies between 1 and 2.5, by IEEE standards (identify), for islanding detection under conditions of zero power mismatch.

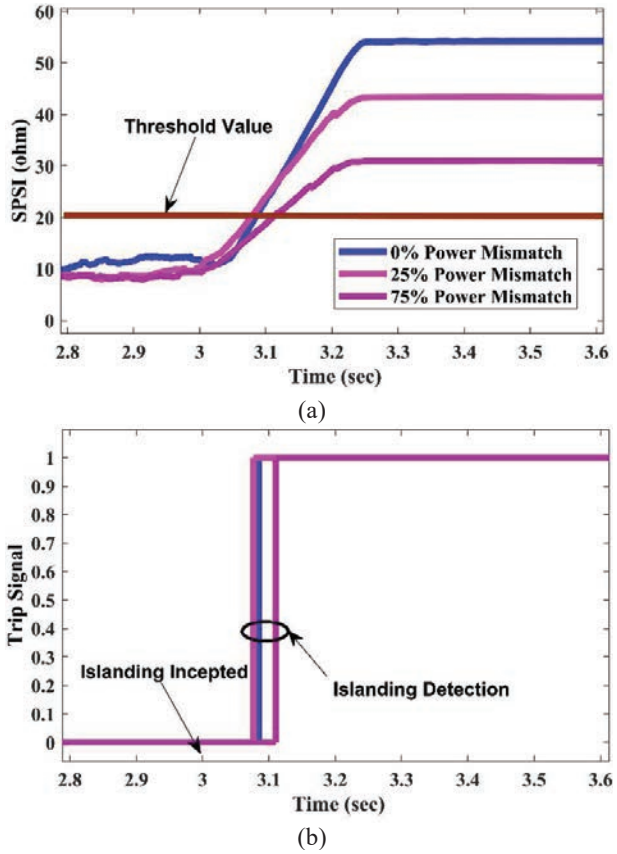

Figure 11 Islanding at various positive power mismatch (a) SPSI (b) Trip signal.

From Figure 13(a), the magnitude of SPSI variation for various quality factors (1, 1.8, and 2.5) exceeds the predefined threshold limit. As demonstrated in Figure 13(b), the suggested algorithm detects islanding and generates a trip signal for the circuit breaker execution. As the value of the quality factor increases, the difference between grid-linked and islanding modes decreases.

4.2 Non-islanding Cases

4.2.1 Resistive load switching

In this section, the impact of an abrupt load switching is assessed. At time instance t = 3 s, the 3 MW load is switched. The load demand is 11.5 MW before t = 3 s, and it increased (14.5 MW) and decreased (8.5 MW) after

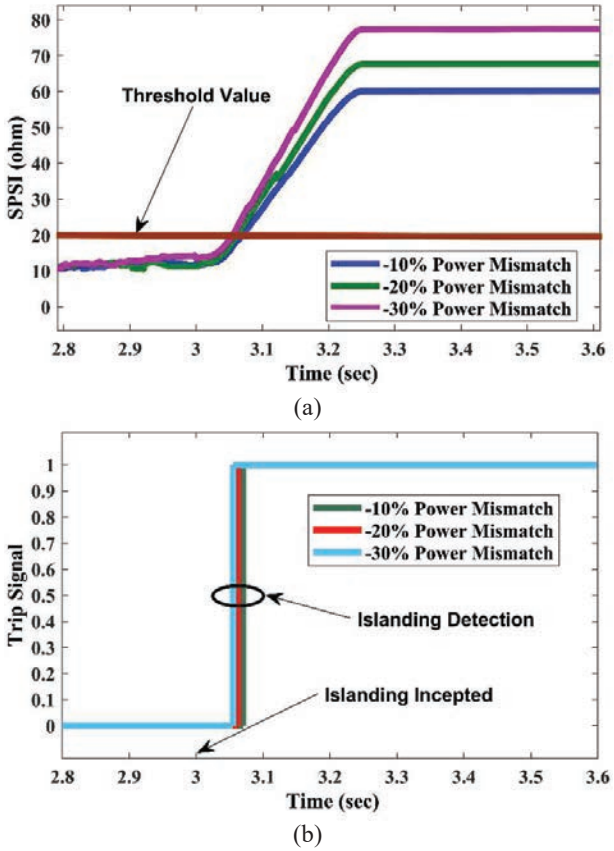

Figure 12 Islanding at various negative power mismatch (a) SPSI (b) Trip signal.

load switching. The variations in SPSI and the trip signal at the instant of load shifting are depicted in Figure 14. According to Figure 14(a) the maximum magnitude of the SPSI in both cases is 12 and 13 Ω, which is less than the threshold limit (20 Ω). Hence, it fails to produce a trip signal, as shown in Figure 14(b).

4.2.2 Capacitor load switching

For power factor correction, voltage sag compensation, and other purposes, capacitors that are linked in parallel to the power system are frequently used. In this case, evaluate the performance of the proposed scheme. When capacitors switch on or off in the microgrid test network at t = 3 s, the variation in SPSI and trip signal are presented in Figure 15. As demonstrated

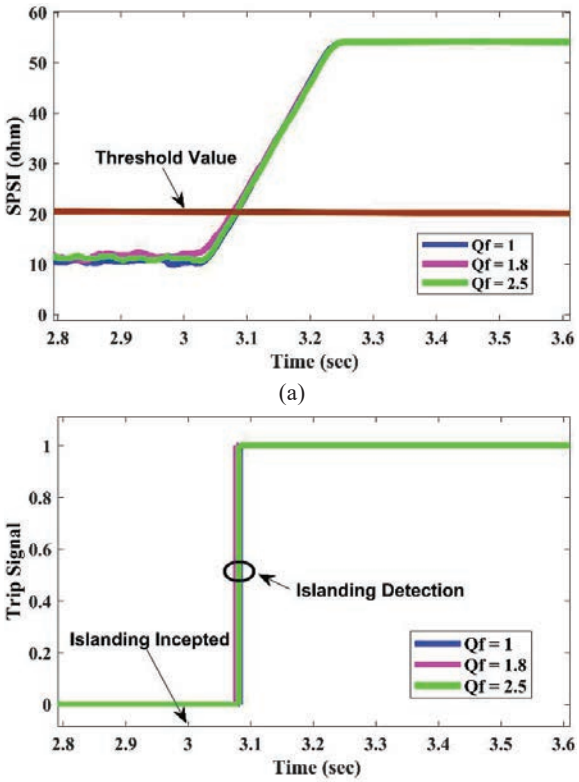

Figure 13 Islanding at various quality factors (a) SPSI (b) Trip signal.

in Figure 15(a), the magnitude of SPSI in both events is less than the threshold value (20 Ω). Therefore, the logic does not generate a trip signal, as shown in Figure 15(b). Therefore, it is a non-islanding event.

4.2.3 Inductive load switching

For inductive load switching, the suggested scheme's efficiency is evaluated. A 3 MVAR inductive load switches in the multi-bus system at t = 3 s. Figure 16 depicts the variations in the SPSI and trip signal caused by the inductive load. In such a case, the SPSI is very low and unable to cross the threshold value, as presented in Figure 16(a). Hence, no generated trip signal, as illustrated in Figure 16(b). Additionally in this instance, the suggested approach delivers precise and admirable results.

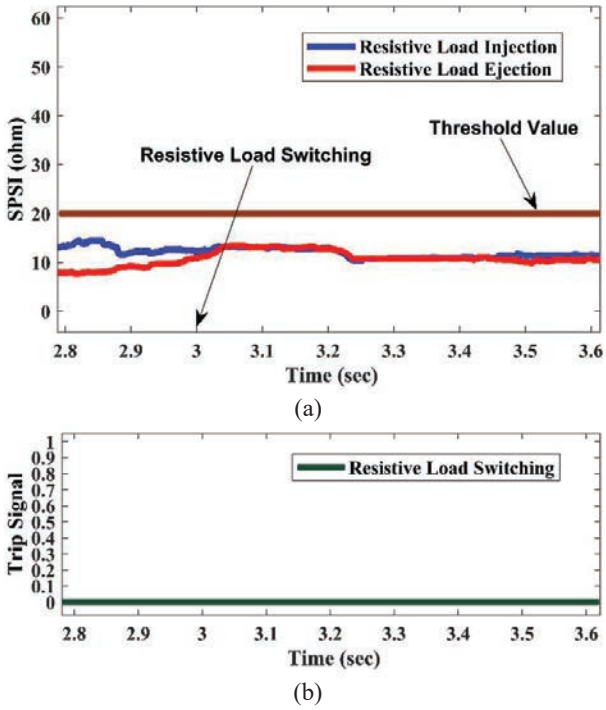

Figure 14 Non-islanding for resistive load switching (a) SPSI (b) Trip signal.

4.2.4 Fault switching

It is important to understand voltage deviations for different fault types, such as LG, LL, LLG, LLL, and LLLG. In time instance t = 3 s, the fault with $R_f = 0.1\ \Omega$ occurs at DG's terminal. According to Figure 17(a), the SPSI response across all fault cases appears lower than the specified threshold. As a result, the proposed approach fails to detect the islanding situation. The trip signal status is zero, as shown in Figure 17(b), indicating the degree of success of the proposed method in the non-islanding situation.

4.2.5 Non-linear load switching

To evaluate the effectiveness of the proposed technique, a three-phase non-linear diode bridge rectifier load with a 2.5 MW rating is switched in the test network at t = 3 s. Harmonics are produced in the power system due to non-linear load switching. From Figure 18(a), the value of SPSI does not exceed the predefined threshold. In the above scenario, IDT fails to produce a trip signal, as demonstrated in Figure 18(b). It is a non-islanding event.

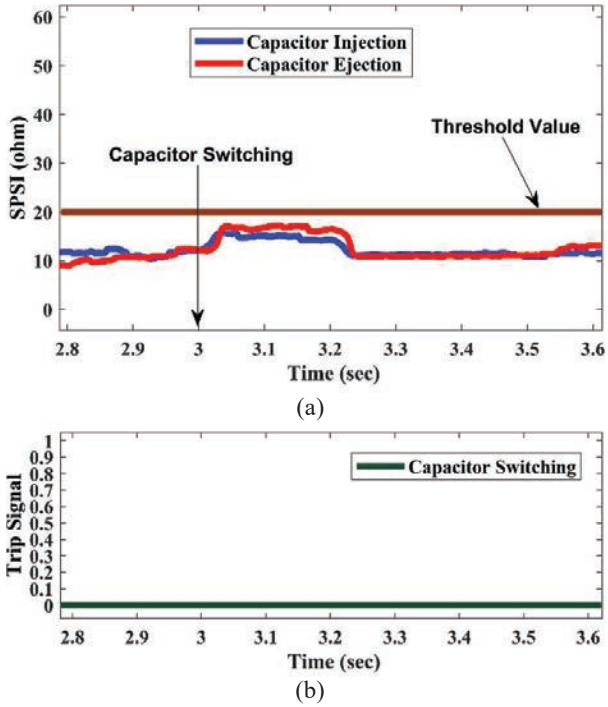

Figure 15 Non-islanding for capacitor load (a) SPSI (b) Trip signal.

4.2.6 Tripping of the distribution generation

The SDG with a 3.5 MVA tripped from the microgrid test network at t = 3 s for zero power mismatch condition. It is observed from Figure 19(a) that the response of SPSI does not exceed the threshold limit. According to Figure 19(b), the proposed scheme fails to produce a trip signal and islanding cannot be detected. It is a non-islanding event.

4.2.7 Effect of the noise signal

In this section, the performance of the proposed scheme is verified in the presence of noise voltage and current signals. The simulation study of the proposed algorithm employs a signal-to-noise ratio (SNR) of 40 dB. It is observed from Figure 20(a) that the response of SPSI variation is less than the threshold limit. Hence, the proposed method fails to detect islanding, and the generation trip signal is zero, as shown in Figure 20(b).

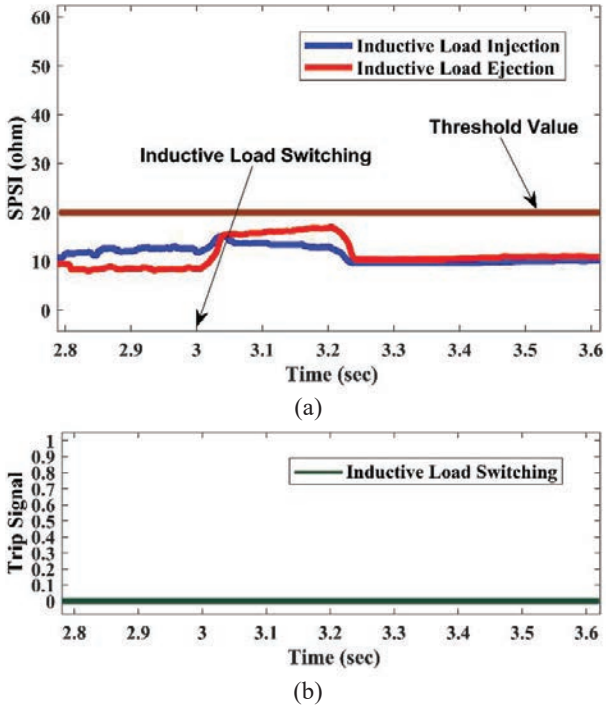

Figure 16 Non-islanding for the inductive load (a) SPSI (b) Trip signal.

4.2.8 To test the effectiveness of the suggested method on an adapted IEEE-13 bus system

A modified IEEE-13 bus system, shown in Figure 21, has been used to test the effectiveness of the proposed algorithm. A modified IEEE 13 bus system includes two DGs. One synchronous diesel (DG_1)-based DG is attached to bus 675. Another wind turbine (DG_2) based DGs are installed on bus 646, respectively. In the microgrid system, a single line-to-ground fault with a fault resistance of $R_f = 0.1\ \Omega$ occurs at bus 650. The islanding is incepted at $t = 3$ s. Figure 22 illustrates the simulation outcomes of SPSI for non-islanding and islanding events at 0% power mismatch. The magnitude of the SPSI exceeds the threshold during islanding events but stays below it during non-islanding events. Hence, the suggested islanding detection method effectively distinguishes between islanding and non-islanding cases in various system conditions.

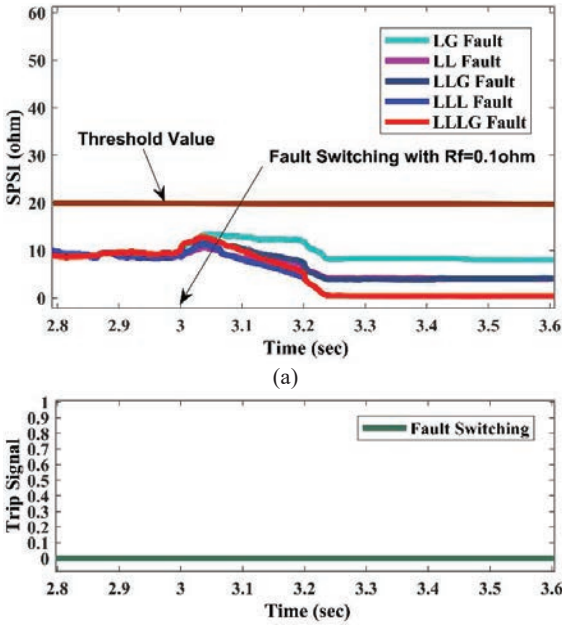

Figure 17 Non-islanding for fault switching (a) SPSI (b) Trip signal.

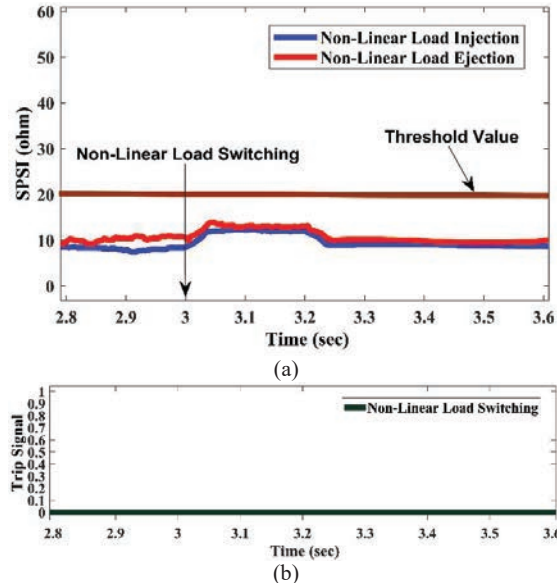

Figure 18 Non-islanding for non-linear load (a) SPSI (b) Trip signal.

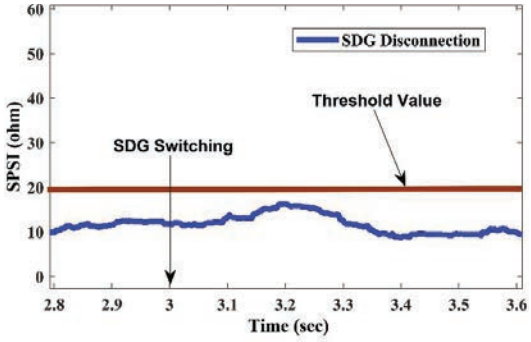

(a)

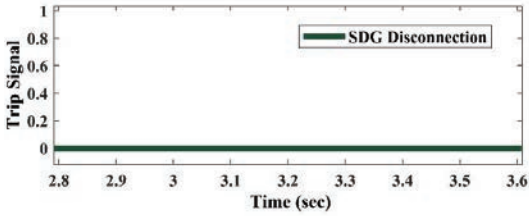

(b)

Figure 19 Non-islanding for DG tripping (a) SPSI (b) Trip signal.

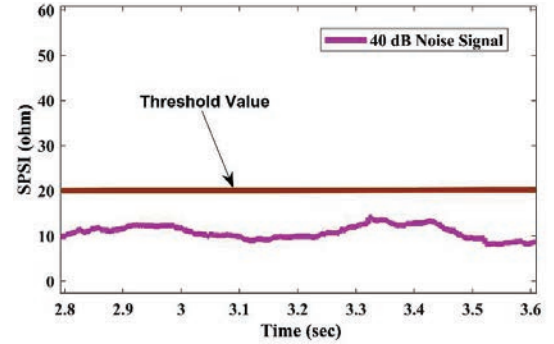

(a)

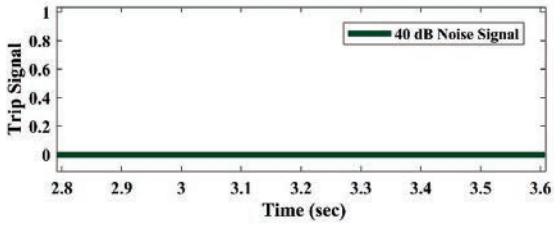

(b)

Figure 20 Non-islanding for noise signal (a) SPSI (b) Trip signal.

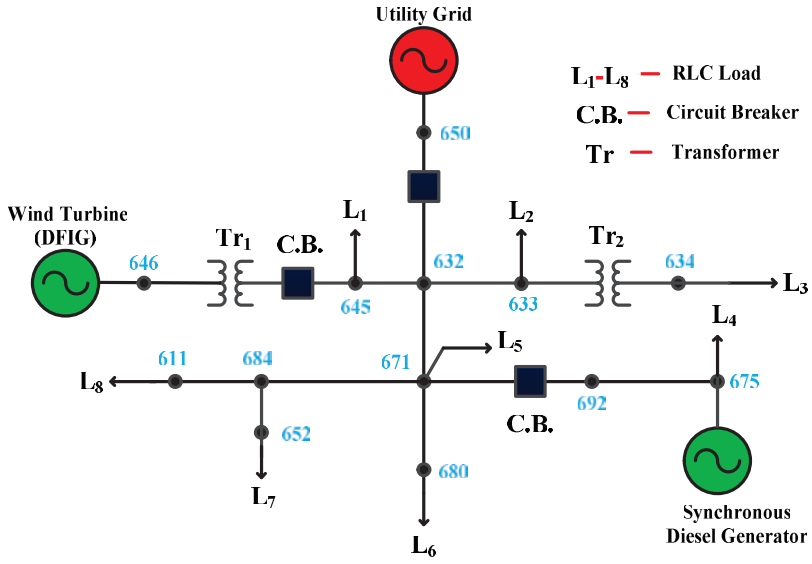

Figure 21 A modified IEEE 13 bus microgrid.

5 Comparative Study of the Proposed Technique

In this section, Table 2 provides an analysis of the proposed approach with the existing islanding techniques [18, 19]. The effectiveness of the proposed scheme analysis by comparison with the Rate of change of frequency (ROCOF) and rate of change of positive sequence voltage (ROCOPSV) methods for islanding events at zero power mismatch conditions. From Figure 23, the magnitude of ROCOF (Hz/s) does not cross the threshold value at zero power mismatch (ZPM). It is not detecting islanding at ZPM. Whereas the proposed method detects islanding at ZPM, as shown in Figure 11. The proposed algorithm is compared to existing schemes [18, 19] for a non-islanding event involving a single line to ground fault with fault resistance $R_f = 0.1\ \Omega$ switching in a multi-bus system at $t = 3$ s. According to Figure 23, the response of ROCOF and ROCOPSV exceeds the predefined threshold. Therefore, the conventional passive techniques fail to identify a non-islanding event at a low value of fault resistance. Whereas the proposed algorithm quickly identifies non-islanding events at low values of fault resistance. It is clear from this comparison that the scheme is better than those proposed in [18] and [19]. The third method [29] identifies islanding by checking if the peak value of the angle of positive sequence voltage (APSV) is smaller

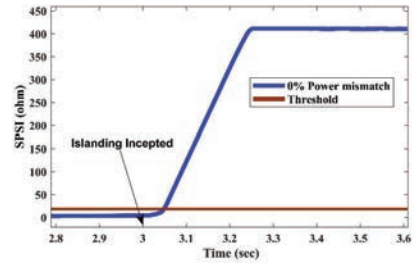

(a)

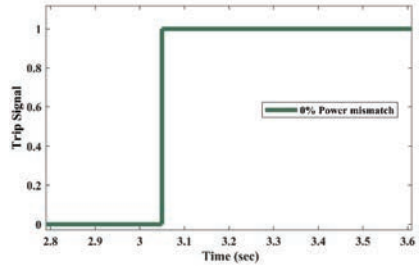

(b)

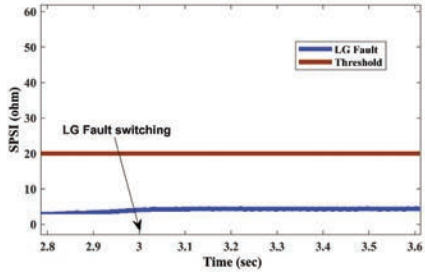

(c)

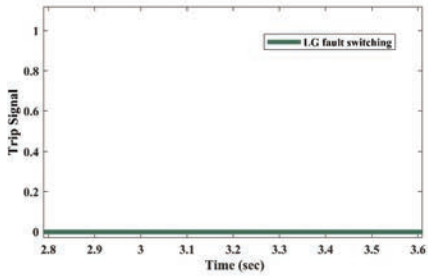

(d)

Figure 22 Islanding event (a) SPSI (b) Trip signal, Non-islanding events (c) SPSI (d) Trip signal.

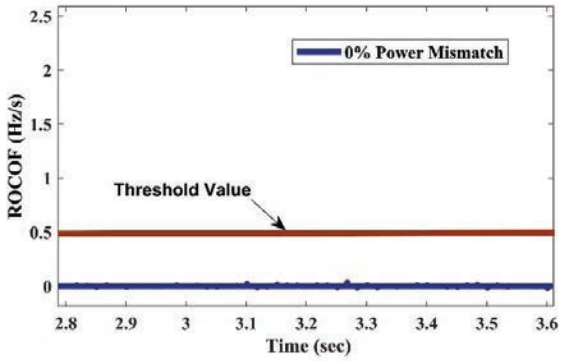

(a)

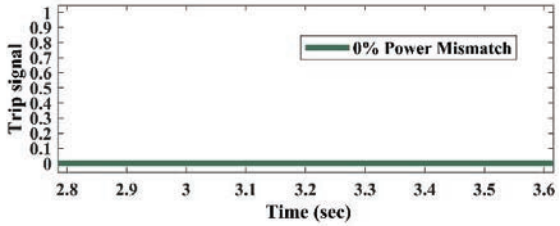

(b)

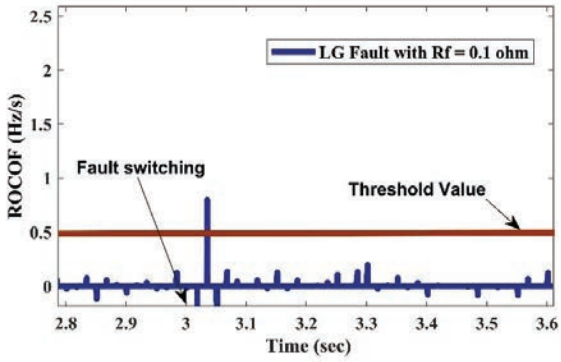

(c)

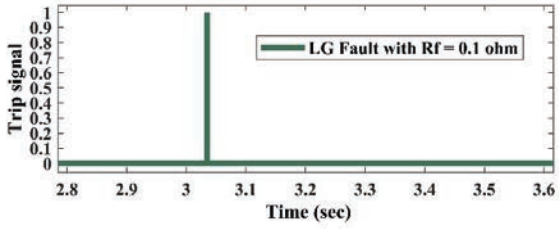

(d)

Figure 23 Continued

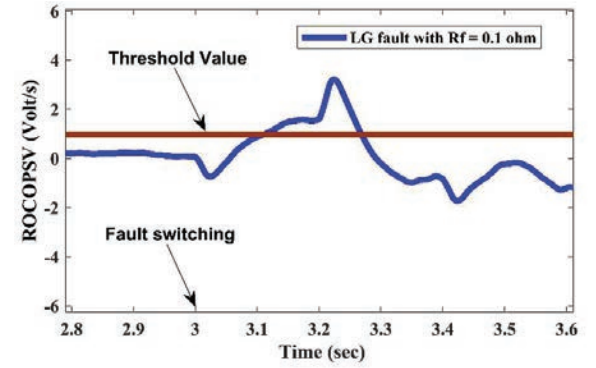

(e)

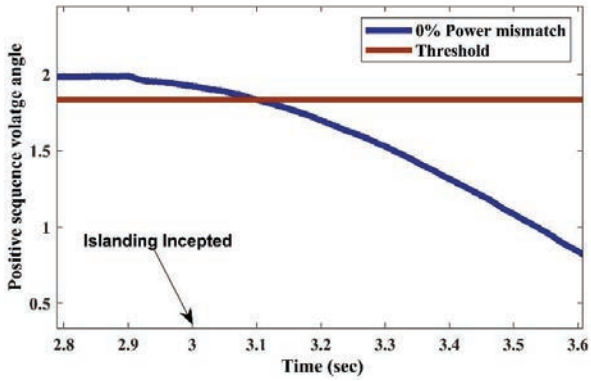

(f)

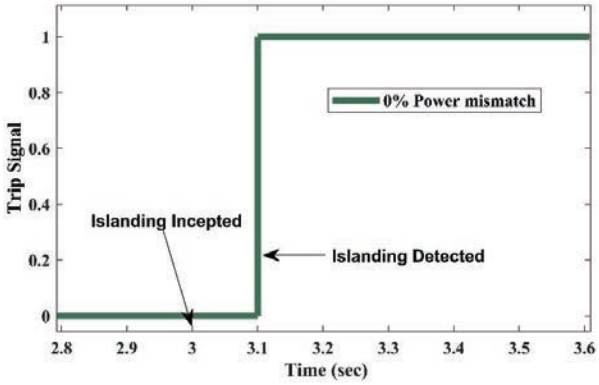

(g)

Figure 23 Comparison of the proposed scheme with ROCOF and ROCOPSV for islanding (a) ROCOF (b) Trip signal, and non-islanding events (c) ROCOF (d) Trip signal (e) ROCOPSV (f) PSVA (g) Trip signal.

Table 2 A comparison of the proposed approach with existing approaches

Ref.	Islanding Methods	NDZ (%)	Detection Time (ms)	Power Quality Issue	Fault (Rf = 0.1Ω)	CS	NLL	Noise	Application Multiple DG
[18]	Rate of change of frequency	17	337	No	×	√	–	×	√
[19]	ROCOPSV	0	10	No	×	√	–	×	√
[20]	DWT	0	26	No	–	√	×	×	√
[21]	TMF	1	55	No	×	√	–	√	–
[22]	ROCONSV	25	250	Yes	–	√	√	×	√
[23]	ROCOV/ ROCOAP	–	200	Yes	×	√	×	√	×
[24]	Maximum Power Point Tracking Injection	0.8	200–300	No	×	√	–	–	√
[25]	Rate of change of voltage and parallel inductive impedance switching	0	300	No	√	√	–	–	√
[26]	Rate of change of voltage and the ratio of voltage and current magnitudes	0.5	108–149	No	×	√	×	×	√
[27]	Active slip frequency	0	225	Yes	×	√	×	×	√
[28]	Difference in positive sequence superimposed impedance angle	Small	23.62	No	–	√	√	×	√
[29]	Positive sequence voltage angle	0	100	No	×	√	–	–	×
	Proposed Technique	0	84	No	√	√	√	√	√

"√" = Verified, "– " = Not considered, "×" = Invalid, CS = Capacitor Switching, NLL = Non-Linear Load.

than the threshold. This is shown in Figure 23(f). The identification process takes 100 ms, which is longer than the suggested scheme (SPSI), as seen in Figure 23(g). In AC microgrids, islanding detection is still in the infancy stage. The following advantages of the proposed scheme are listed below:

- It correctly detects islanding within 84 ms, which fulfills IEEE Std. 1547-2018 criteria.
- This scheme identifies islanding at zero power mismatch conditions.
- The proposed scheme operates well in both converter and synchronous-based generators.
- The proposed scheme is resilient to short circuit faults, load switching, and stable/unstable power fluctuations.
- It is suitable for both multi-bus and standard IEEE 13 bus systems.

The proposed approach has some challenges, as listed below:

- The suggested technique's threshold depends on the system topology.
- This scheme is maloperation in single pole tripping.

6 Conclusion

This article proposes a novel passive islanding detection technique based on SPSI for multi-bus systems to detect islanding more effectively. This work evaluates the performance of the proposed algorithm under various islanding and non-islanding scenarios. The islanding events like power mismatch, quality factor, and non-islanding events like load switching, capacitor switching, inductive load switching, and fault switching are taken care of by the proposed technique. The proposed scheme also performs well in challenging conditions like noise and DG tripping. The outcomes acquired during the comparative study of the proposed method with the existing technique indicate that the proposed method is better, robust, and easy to implement. The proposed IDT is superior to all other IDTs and microgrid networks. All conditions are successfully verified by the proposed approach. This research focuses only on wind power and synchronous-based distributed generation (DG). However, the islanding technique proposed can also be applied efficiently to microgrids that include other kinds of DGs, such as solar power and fuel cell-based DGs, and there should be further investigation on the stability of the proposed method during various types of system disturbance events.

References

[1] Mohammed Ali Khan, Ahteshamul Haque, V.S. Bharath Kurukuru, Mekhilef Saad, "Islanding detection techniques for grid-connected photovoltaic systems-A review," Renewable and Sustainable Energy Reviews 2022. doi: 10.1016/j.rser.2021.111854.

[2] M. Sujikannan, A. R. Kumar, and S. A. Daniel, "Sizing of Rooftop PV Array and Community-Run Battery Storage for an Energy Cooperative in Prosumer Cluster", DGAEJ, vol. 37, no. 06, pp. 1797–1822, Oct. 2022, doi: 10.13052/dgaej2156-3306.3764.

[3] "IEEE Standard for Interconnection and Interoperability of Distributed Energy Resources with Associated Electric Power Systems Interfaces–Amendment 1: To Provide More Flexibility for Adoption of Abnormal Operating Performance Category III," in IEEE Std 1547a-2020 (Amendment to IEEE Std 1547-2018), vol., no., pp. 1–16, 15 April 2020, doi: 10.1109/IEEESTD.2020.9069495.

[4] I. P. Bharti, N. K. Singh, O. H. Gupta and A. K. Singh, "Developments in Islanding Detection and Its Comparison: A Comprehensive Review," 2021 IEEE 8th Uttar Pradesh Section International Conference on Electrical, Electronics and Computer Engineering (UPCON), Dehradun, India, 2021, pp. 1–10, doi: 10.1109/UPCON52273.2021.9667656.

[5] H. Abdi, A. Rostami, and N. Rezaei, "A novel passive islanding detection scheme for synchronous-type DG using load angle and mechanical power parameters," Electrical. Power System. Res., vol. 192, Mar. 2021. doi: 10.1016/j.epsr.2020.106968.

[6] Nikita Gupta, Rahul Dogra, Rachana Garg & Parmod Kumar, "Review of islanding detection schemes for utility-interactive solar photovoltaic systems," International Journal of Green Energy 2022. doi: 10.1080/15435075.2021.1941048.

[7] A. Hussain, C.-H. Kim and A. Mehdi, "A Comprehensive Review of Intelligent Islanding Schemes and Feature Selection Techniques for Distributed Generation System," in IEEE Access, vol. 9, pp. 146603–146624, 2021. doi: 10.1109/ACCESS.2021.3123382.

[8] J. Bashir, and P. Jena, "Positive Sequence Superimposed Based Islanding Detection Method Used in Distributed Generation," Distributed Generation & Amp, Alternative Energy Journal, 38(02), 367–392, 2023. doi: 10.13052/dgaej2156-3306.3821.

[9] Fadila Barkat, Ali Cheknane, Josep M. Guerrero, Abderezak Lashab, Marcel Istrate, Mihai Gavrilas, Justina G. Motas, Ioan Viorel Banu,

"Review, analysis, and performance evaluation of the most common four active methods for islanding detection in grid-connected photovoltaic systems," Electric Power Systems Research, 2023. doi: 10.1016/j.epsr.2022.108909.

[10] A. Pouryekta, and V. K. Ramachandaramurthy, "A Hybrid Islanding Detection Method for Distribution Systems," Distributed Generation &Amp; Alternative Energy Journal, 33(4), 44–67, 2018. doi: 10.13052/dgaej2156-3306.3343.

[11] G. Wang, F. Gao, J. Liu, Q. Li, and Y. Zhao, "Design consideration and performance analysis of a hybrid islanding detection method combining voltage unbalance/total harmonic distortion and bilateral reactive power variation," in CPSS Transactions on Power Electronics and Applications, vol. 5, no. 1, pp. 86–100, March 2020, doi: 10.24295/CPSSTPEA.2020.00008.

[12] K.-L. Chen, Y. Guo, J. Wang, and X. Yang, "Contactless Islanding Detection Method Using Electric Field Sensors," in IEEE Transactions on Instrumentation and Measurement, vol. 70, pp. 1–13, Art no. 9001413, 2021. doi: 10.1109/TIM.2020.3043096.

[13] W. Xu, G. Zhang, C. Li, W. Wang, G. Wang, and J. Kliber, "A Power Line Signaling Based Technique for Anti-islanding Protection of Distributed Generators: Part I: Scheme and Analysis," IEEE Power Engineering Society General Meeting, Tampa, FL, USA, pp. 1–1, 2007. doi: 10.1109/PES.2007.385448.

[14] C.-I. Chen and Y.-C. Chen, "Intelligent Identification of Voltage Variation Events Based on IEEE Std 1159-2009 for SCADA of Distributed Energy System," IEEE Transactions on Industrial Electronics, vol. 62, no. 4, pp. 2604–2611, April 2015. doi: 10.1109/TIE.2014.2348948.

[15] D. Mlakiæ, H. R. Baghaee and S. Nikolovski, "Gibbs Phenomenon-Based Hybrid Islanding Detection Strategy for VSC-Based Microgrids Using Frequency Shift, THDU, and RMSU," IEEE Transactions on Smart Grid, vol. 10, no. 5, pp. 5479–5491, Sept. 2019, doi: 10.1109/TSG.2018.2883595.

[16] S. Barczentewicz, T. Lerch, A. Bie, and K. Duda, "Laboratory evaluation of a phasor-based islanding detection method," Energies, vol. 14, no. 7, p. 1953, Apr. 2021. doi: 10.3390/en14071953.

[17] Pravin Kumar, Vishal Kumar, Barjeev Tyagi, "Islanding detection for a reconfigurable microgrid with RES," IET Generation, Transmission & Distribution 2020. doi: 10.1049/gtd2.12095.

[18] C. Li, C. Cao, Y. Cao, Y. Kuang, L. Zeng, and B. Fang, "A review of islanding detection methods for microgrid," Renewable Sustain. Energy Rev., vol. 35, pp. 211–220, 2014. doi: 10.1016/j.rser.2014.04.026.

[19] Ch. Rami Reddy, K. Harinadha Reddy, "An Efficient Passive Islanding Detection Method for Integrated DG System with Zero NDZ," International Journal of Renewable Energy Research, December 2018. doi:10.20508/ijrer.v8i4.8335.g7507.

[20] H. Shayeghi and B. Sobhani, "Zero NDZ assessment for anti-islanding protection using wavelet analysis and neuro-fuzzy system in inverter-based distributed generation," Energy Convers. Manage., vol. 79, pp. 616–625, Mar. 2014. doi: 10.1016/j.enconman.2013.12.062.

[21] R. Dubey, M. Popov, and S. R. Samantaray, "Transient monitoring function-based islanding detection in the power distribution network," IET Generation., Transmission. Distribution., vol. 13, no. 6, pp. 805–813, Mar. 2019. doi: 10.1049/iet-gtd.2017.1941.

[22] O. H. Gupta, M. Tripathy, V. K. Sood, "Islanding detection scheme for converter-based DGs with nearly zero non-detectable zone," IET Generation Transmission Distribution 13(23):5365–5374, 2019. doi: 10.1049/iet-gtd.2018.5168.

[23] M. Seyedi, S. A. Taher, B. Ganji, and J. Guerrero, "A Hybrid Islanding Detection Method Based on the Rates of Changes in Voltage and Active Power for the Multi-Inverter Systems," in IEEE Transactions on Smart Grid, vol. 12, no. 4, pp. 2800–2811, July 2021. doi: 10.1109/TSG.2021.3061567.

[24] R. Bakhshi-Jafarabadi, J. Sadeh and M. Popov, "Maximum Power Point Tracking Injection Method for Islanding Detection of Grid-Connected Photovoltaic Systems in Microgrid," IEEE Transactions on Power Delivery, vol. 36, no. 1, pp. 168–179, Feb 2021, doi: 10.1109/TPWRD.2020.2976739.

[25] A. Rostami, A. Jalilian, S. Zabihi, J. Olamaei, and E. Pouresmaeil, "Islanding Detection of Distributed Generation Based on Parallel Inductive Impedance Switching," IEEE Systems Journal, vol. 14, no. 1, pp. 813–823, March 2020, doi: 10.1109/JSYST.2019.2923289.

[26] Karimi, Mazaher, Mohammad Farshad, Qiteng Hong, Hannu Laaksonen, and Kimmo Kauhaniemi, "An Islanding Detection Technique for Inverter-Based Distributed Generation in Microgrids," Energies 14, no. 1: 130, 2021, doi: 10.3390/en14010130.

[27] P. K. Ganivada and P. Jena, "Active Slip Frequency Based Islanding Detection Technique for Grid-Tied Inverters," IEEE Transactions on

Industrial Informatics, vol. 16, no. 7, pp. 4615–4626, July 2020, doi: 10.1109/TII.2019.2949009.

[28] Ruchita Nale, Monalisa Biswal, Nand Kishor, "A passive communication-based islanding detection technique for AC microgrids," International Journal of Electrical Power & Energy Systems, 2022, doi: 10.1016/j.ijepes.2021.107657.

[29] Nouman Shafique, Safdar Raza, Sumayya Bibi, Muhammad Farhan, Mughees Riaz, "A simplified passive islanding detection technique based on susceptible power indices with zero NDZ," Ain Shams Engineering Journal, Volume 13, 2022, doi: 10.1016/j.asej.2021.11.006.

Biographies

Indradeo Pratap Bharti received his B.Tech degree in electrical engineering from Gurukul Kangri University, Haridwar, India, in 2014, and his M.Tech degree in power systems from the Indian Institute of Technology (ISM), Dhanbad, India, in 2016. Currently, he is pursuing a Ph.D. degree at the Motilal Nehru National Institute of Technology Allahabad, Prayagraj, India, His research interests include electric power systems, power distribution systems, and islanding operations in microgrids.

Navneet Kumar Singh received his B.Sc. Engineering degree in Electrical Engineering in 2004 and M. Tech degree in 2006 from Dayalbagh

Educational Institute, Agra, India. And Ph.D. degree in 2016 from the Motilal Nehru National Institute of Technology Allahabad, Allahabad, India. He is presently working as an assistant professor in the Department of Electrical Engineering at Motilal Nehru National Institute of Technology Allahabad, Allahabad, India. His major areas of research are Power System Operation and Planning, and Artificial Intelligence Applications in Power Systems.

Om Hari Gupta obtained his Ph.D. degree in electrical engineering from the Indian Institute of Technology Roorkee, Roorkee, India. He is presently employed as an assistant professor in the Department of Electrical Engineering, at the National Institute of Technology Jamshedpur, India. He is a recipient of the Canadian Queen Elizabeth II Diamond Jubilee Scholarship for research visiting the Ontario Tech University (Formerly University of Ontario Institute of Technology), Oshawa, ON, Canada in 2017. His major areas of research interest include power system protection, microgrids, renewable-based distributed generation, and electric power quality. Dr. Gupta is a senior member of IEEE and a reviewer for various international journals including IEEE Transactions on Power Delivery, Electric Power Components and Systems, International Journal of Electrical Power and Energy Systems, etc.

Asheesh Kumar Singh received his B. Tech degree in electrical engineering from Harcourt Butler Technical. Institute, Kanpur (INDIA), in 1991, and the M.Tech. degree in Control systems from the National Institute of Technology (formerly REC), Kurukshetra (INDIA), in 1994. I doctorate from the Indian Institute of Technology, Roorkee (INDIA), in 2007. He is currently working as a Professor with the Department of Electrical Engineering, MNNIT Allahabad. He has more than 15 years of teaching experience. He is also serving as a Chair in Conferences (IEEE-UPCON). His research interests include power Systems, Power quality, E-mobility, Renewable energy integration, Microgrids, and Smart Grid.

Vijay K. Sood received his Ph.D. degree from the University of Bradford, Bradford, U.K., in 1977. He is currently an Associate Professor at OntarioTech University, Oshawa, Canada. He has extensive experience in the simulation of HVDC-FACTS systems and their controllers. He has authored two textbooks on HVDC Transmission. His research focuses on the monitoring, control, and protection of power systems and the integration of renewable energy systems into the smart grid. Dr. Sood is a Registered Professional Engineer in the province of Ontario, a Fellow of the IEEE, Engineering Institute of Canada, and an Emeritus Fellow of the Canadian Academy of Engineering.